Supporting information

High energy density of polyimide films employing imidization reaction kinetics strategy at elevated temperature

Xue-Jie Liu, Ming-Sheng Zheng, Gang Wang, Yi-Yi Zhang, Zhi-Min Dang, George Chen and Jun-Wei Zha**

Table S1 Dianhydride and diamine monomers for synthesizing polyimides

	ODPA-MPD film	PMDA-ODA film	BPDA-BPB film
Dianhydride	ODPA 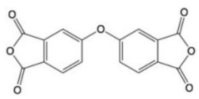	PMDA 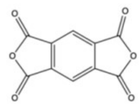	BPDA 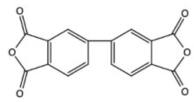
Diamine	MPD 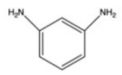	ODA 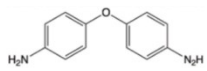	BPB 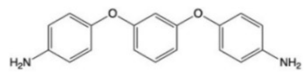

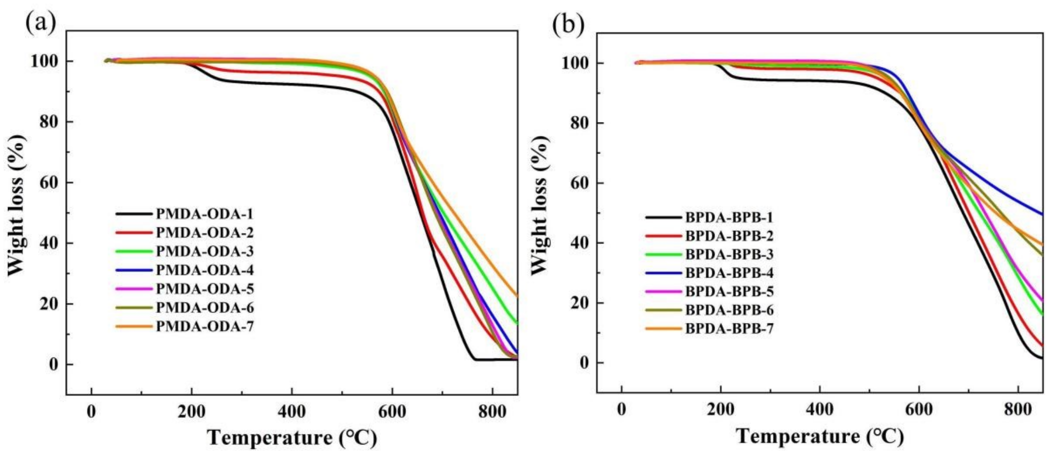

Fig. S1 TGA curves of (a) PMDA-ODA and (b) BPDA-BPB films with different ID.

Table S2 Imidization degree and thermal property of the PMDA-ODA films.

PMDA-ODA	1	2	3	4	5	6	7
ID (%)	20	68	83	89	≈100	≈100	≈100
$T_{d5\%}$ (°C)	240	499	556	564	565	562	565
$T_{d10\%}$ (°C)	528	573	583	587	588	589	587

Table S3 Imidization degree and thermal property of the BPDA-BPB films.

BPDA-BPB	1	2	3	4	5	6	7
ID (%)	10	60	86	≈100	≈100	≈100	≈100
$T_{d5\%}$ (°C)	237	515	534	556	539	540	531
$T_{d10\%}$ (°C)	531	562	567	577	566	567	563

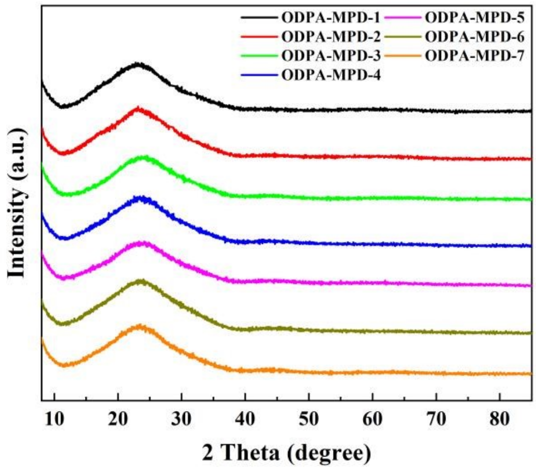

Fig. S2 XRD patterns of the ODPA-MPD films with different ID.

All the ODPA-MPD films had a typical amorphous structure, with a broad peak at 2θ = 23°, which was mainly due to the regular arrangement of PI chains.

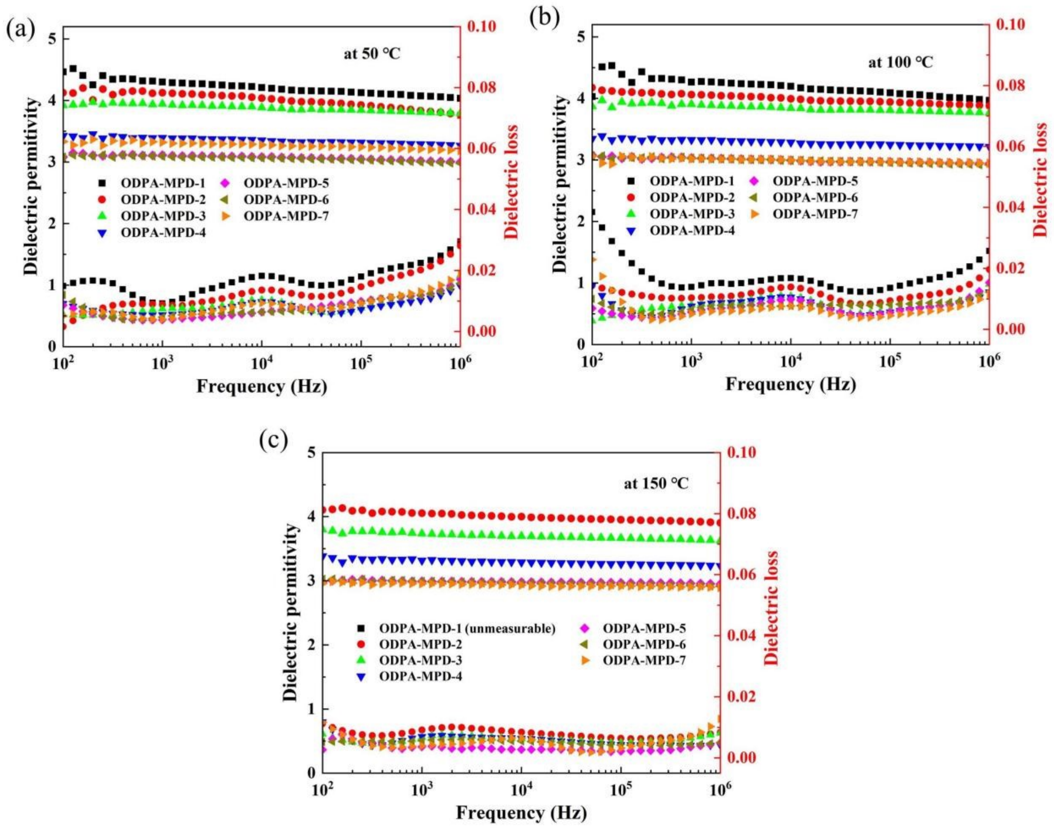

Fig. S3 Frequency-dependent of dielectric permittivity and dielectric loss of ODPA-MPD films with different ID at (a) 50 °C, (b) 100 °C and (c) 150 °C, respectively.

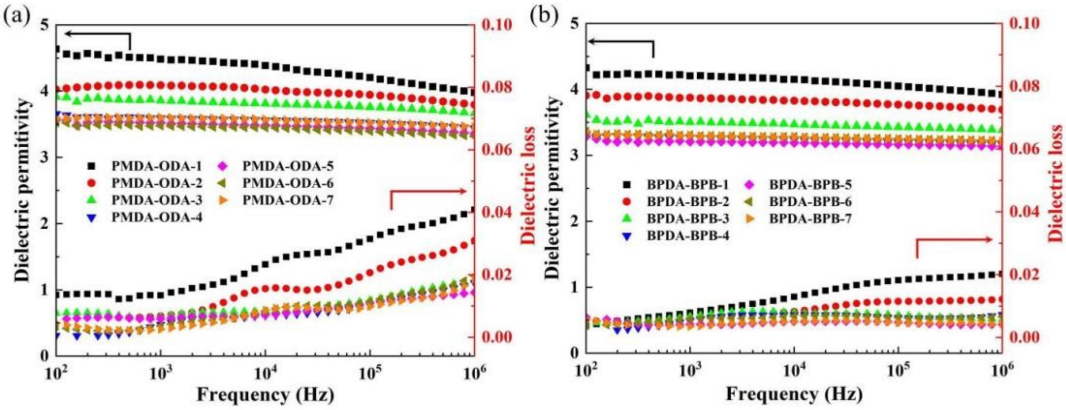

Fig. S4 Frequency-dependent of dielectric permittivity and dielectric loss of (a) PMDA-ODA and (b) BPDA-BPB films with different ID.

The PMDA-ODA-1 and BPDA-BPB-1 films obtained the highest dielectric permittivities of 4.48 and 4.2 at 1kHz, respectively. It was mainly attributed to the fact that they contained the largest number of -COOH and -CONH- polar groups. The dielectric loss became larger with the gradual decrease of ID.

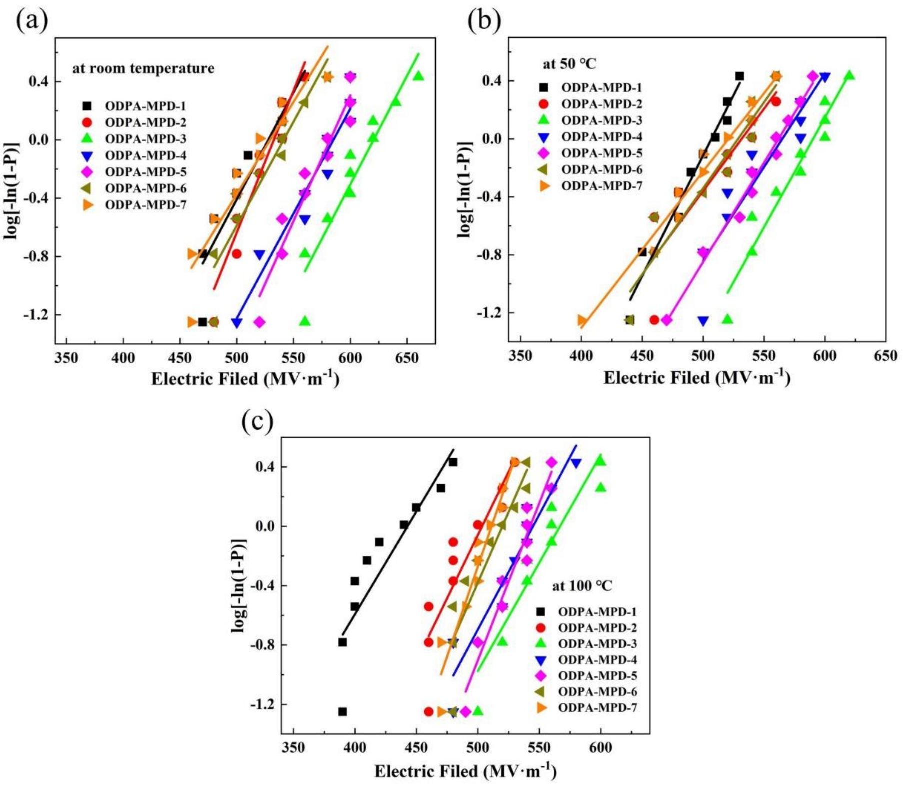

Fig. S5 Weibull distribution of breakdown strength of the ODPA-MPD films with different ID at (a) room temperature, (b) 50 °C and (c) 100 °C, respectively.

The ODPA-MPD-3 film had the highest breakdown strength of 618 MV m^{-1} at room temperature, 595 MV m^{-1} at 50 °C, and 565 MV m^{-1} at 100 °C, respectively.

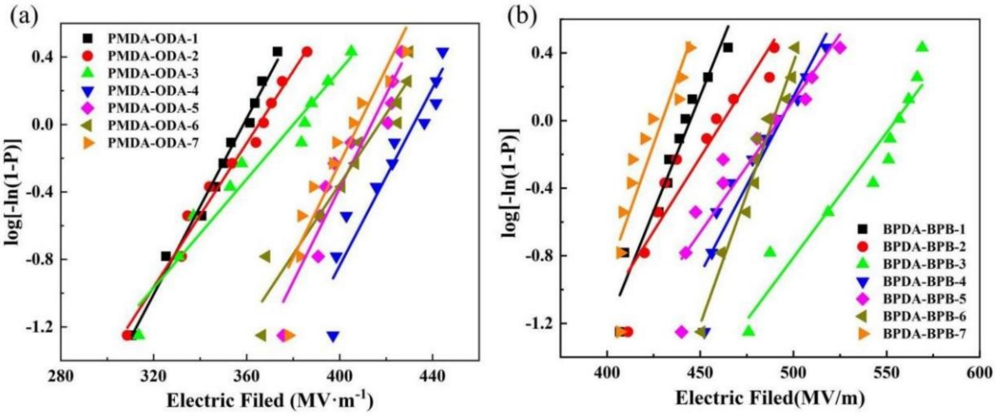

Fig. S6 Weibull distribution of breakdown strength of the (a) PMDA-ODA and (b) BPDA-BPB films with different ID.

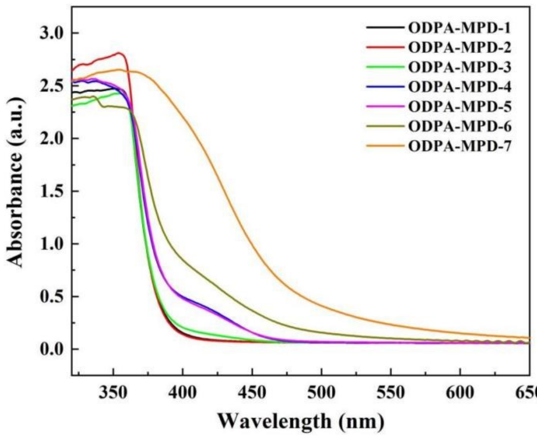

Fig. S7 UV-Vis-NIR diffuse reflection spectroscopy of the ODPA-MPD films with different ID.

Table S4 Bandgap for ODPA-MPD films

ODPA-MPD	1	2	3	4	5	6	7
E_g (eV)	3.27	3.27	3.26	3.21	3.20	3.11	2.57

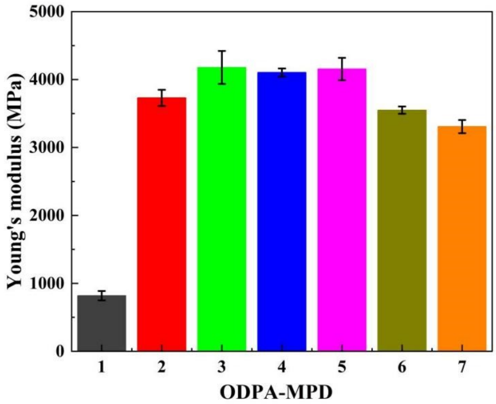

Fig. S8 Young's modulus of the ODPA-MPD films with different ID.

With the increase of ID, the Young's modulus of ODPA-MPD films increased firstly and then decreased. The ODPA-MPD-3~5 films all achieved the highest Young's modulus (~ 4100 MPa).

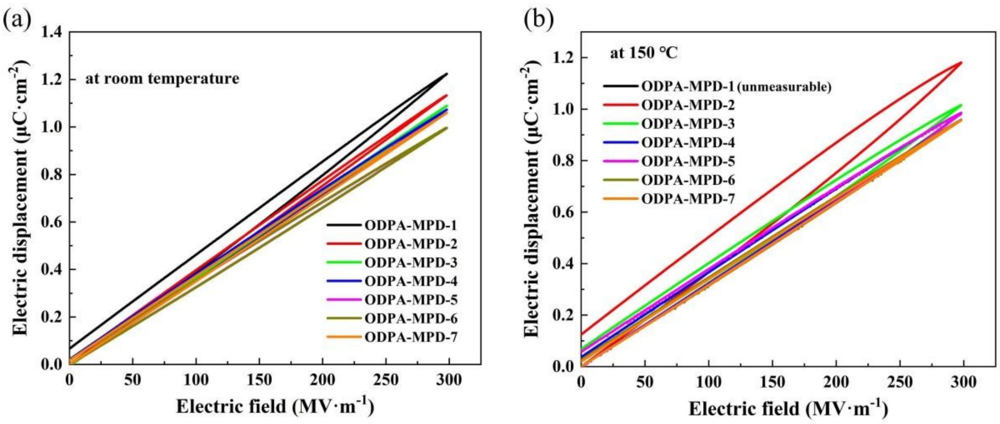

Fig. S9 D-E loops of the ODPA-MPD films (a) at room temperature and (b) at 150 °C under 300 MV m^{-1}.

The D-E loops of the ODPA-MPD films indicated that the electric displacement value gradually decreased as the ID increased. The ODPA-MPD-1 film obtained the highest electric displacement of 1.2 μC cm^{-2} under 300 MV m^{-1} at room temperature. At 150 °C, the ODPA-MPD-2 film had the highest electric displacement value of 1.18 μC cm^{-2} under 300 MV m^{-1}.

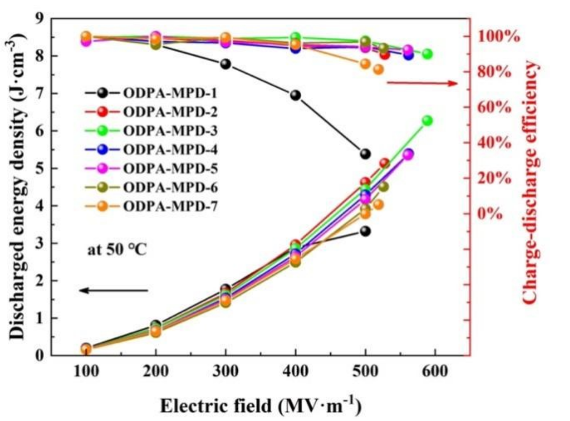

Fig. S10 Discharged energy density and charge-discharge efficiency of the ODPA-MPD films with different ID at 50 °C.

Bipolar carrier transport model

The bipolar charge transport model is used to simulate the injection, migration, trapping, detrapping, and recombination of electrons and holes.[1] When the electric field is less than 100 kV mm^{-1}, the Schottky emission model can describe the charge injection process. The boundary conditions for the injected charges are expressed as follows: [2]

$$J_e(t) = AT^2 exp(-\frac{e\omega_{ei}}{kT}) exp(\frac{e}{kT}\sqrt{\frac{e|E_c(t)|}{4\pi\varepsilon_0\varepsilon_r}}) \tag{1}$$

$$J_h(t) = AT^2 exp(-\frac{e\omega_{hi}}{kT}) exp(\frac{e}{kT}\sqrt{\frac{e|E_a(t)|}{4\pi\varepsilon_0\varepsilon_r}}) \tag{2}$$

where $J_e(t)$ and $J_h(t)$ are the current density induced by electrons and holes at cathode and anode, t is the time, T represents the temperature in kelvin, A is the Richardson constant, ω_{ei} and ω_{hi} are the injection barriers for electrons and holes, e represents the electron charge, and $E_c(t)$ and $E_a(t)$ are the electric field at cathode and anode, respectively. The basic governing equations of the bipolar carrier transport model in the dielectrics mainly include the Poisson equation, current continuity equation, conduction equation as follows:

$$\nabla\cdot(-\varepsilon\nabla\varphi(t)) = \rho(t) \tag{3}$$

$$\frac{\partial\rho(a)}{\partial t} + \nabla\cdot J_a(t) = S_a(t) \tag{4}$$

$$J_a(t) = -\mu_a\rho_a(t)\nabla\varphi(t) \tag{5}$$

where φ represents the electric potential, ρ is the charge density of each carrier, $\boldsymbol{J}$ represents the current density formed by carrier transport, andμ is the carrier mobility. S_a is the source term, where a represents different types of charges, including four terms $S_{e\mu}$, S_{et}, $S_{h\mu}$, S_{ht}. The source terms for the four types of carriers are as follows:

$$S_{e\mu} = -S_1\rho_{ht}\rho_{e\mu} - S_3\rho_{h\mu}\rho_{e\mu} - B_e\rho_{e\mu}\left(1 - \frac{\rho_{et}}{n_{0et}}\right) + D_e\rho_{et} \tag{6}$$

$$S_{et} = -S_2\rho_{h\mu}\rho_{et} - S_0\rho_{ht}\rho_{et} - B_e\rho_{e\mu}\left(1 - \frac{\rho_{et}}{n_{0et}}\right) - D_e\rho_{et} \tag{7}$$

$$S_{h\mu} = -S_2\rho_{h\mu}\rho_{et} - S_3\rho_{h\mu}\rho_{e\mu} - B_e\rho_{h\mu}\left(1 - \frac{\rho_{ht}}{n_{0ht}}\right) + D_h\rho_{ht} \tag{8}$$

$$S_{ht} = -S_1\rho_{h\mu}\rho_{et} - S_0\rho_{ht}\rho_{et} - B_e\rho_{h\mu}\left(1 - \frac{\rho_{ht}}{n_{0ht}}\right) - D_h\rho_{ht} \tag{9}$$

$$D_{e,h} = \nu\cdot exp(\frac{\omega_{et,ht}}{kT}) \tag{10}$$

where S_0, S_1, S_2, and S_3 represent the recombination coefficient of hetero-polar carriers, B_e and B_h are the trapping coefficients for electrons and holes, n_{0et} and n_{0ht} are the concentration of electron traps and hole traps, $D_{e,h}$ is detrapping rate of trapped electrons and trapped holes, v is escape frequency, and $\omega_{et,ht}$ is barrier height of electron traps and hole traps.

Table S5. Parameters for the bipolar carrier transport model simulation

parameters	ODPA-MPD-2	ODPA-MPD-3	ODPA-MPD-5
$B_{e,\,h}$	0.1 S^{-1}	0.1 S^{-1}	0.1 S^{-1}
$n_{0et,\,ht}$	2.59×10^{22} eV^{-1} m^{-3}	3.65×10^{22} eV^{-1} m^{-3}	2.67×10^{22} eV^{-1} m^{-3}
$\omega_{et,\,ht}$	0.82 eV	0.86 eV	0.87 eV
S_0, S_1, S_2	6.4×10^{-22} m^2 C^{-1} s^{-1}	6.4×10^{-22} m^2 C^{-1} s^{-1}	6.4×10^{-22} m^2 C^{-1} s^{-1}
S_3	0 m^2 C^{-1} s^{-1}	0 m^2 C^{-1} s^{-1}	0 m^2 C^{-1} s^{-1}
$\omega_{ei,\,hi}$	1.2 eV	1.2 eV	1.2 eV
E	50 MV m^{-1}	50 MV m^{-1}	50 MV m^{-1}
ε_r	4.39	4.06	3.31
T	298 K	298 K	298 K

References

1 J. F. Zhang, Q. G. Chen, M. H. Chi, P. Tan, W. X. Sun and J. M. Cao, *IEEE Trans. Dielectr. Electr. Insul.* 2019, **26**, 1334.

2 S. Jin, J. J. Ruan, Z. Y. Du, G. D. Huang, L. Zhu, W. M. Guan, Z. F. Yang and L. Y. Li, *IEEE Trans. Magn.* 2016, **52**, 1.